Chapter – 3

Development of New Empirical Formula for (γ, n) reaction cross section near to GDR Peak

---

Publication related to this chapter:

Rajnikant Makwana, S. Mukherjee, Jian-Song Wang, and Zhi-Qiang Chen, "New empirical formula for (γ, n) reaction cross section near GDR Peak for elements with Z >60",

Chinese Physics C Vol. 41, No. 4 (2017) 044105

Impact Factor 5.084

3.1. Introduction

Photonuclear reactions are becoming more important for the fusion reactors and accelerator driven sub-critical system (ADS), where high-energy photons will be generated and subsequently interact with the materials. The study of (γ, n) reactions is important for a variety of current and emerging fields, such as radiation shielding design, radiation transport, absorbed dose calculations for medical, physics, technology of fusion-fission reactors, nuclear transmutation and waste management applications [1,2]. In a fusion reactor, during the plasma shot, de-confined runaway electrons can interact with the first wall of the reactor and can produce high energy photons [3]. As a photon is a massless particle and its interaction is different than the neutron, and the mechanism is energy dependent. The high energetic photon can open reaction channels like (γ, n), (γ, p), (γ, 2n), (γ, 3n), etc. The most prominent reaction is (γ, n), as it has the lowest threshold than multi-neutron emission, whereas for charged particle emission the Coulomb barrier needs to be considered. Exact information about the cross section of such nuclear reaction is needed in order to perform accurate nuclear transport calculations. Tungsten (W) and beryllium (Be) are selected as first wall materials for the fusion reactor- International Thermonuclear Experimental Reactor (ITER) [4]. Among tungsten isotopes, only ^{182}W (26.5 %), ^{184}W (30.64%) and ^{186}W (28.43%) have experimental cross section data for (γ, n) reaction. It is necessary to have the cross section of (γ, n) reaction for ^{180}W (0.12%) and ^{183}W (14.31%) along with all the remaining long-lived unstable isotopes, as they will interact with high-energy photons during the confined runaways and disruption phase [5]. Gamma induced nuclear reaction are also important for the nuclear transmutation (e.g. ^{234}U(γ, n)^{233}U), which is useful for the nuclear safety and incineration. The importance of the gamma incineration technique has been studied in the case of many isotopes for nuclear waste management [6-8].

In ADSs, the high energy proton beam will interact with high Z elements such as W, Pb-Bi, Th, and U, which will produce neutrons through spallation reactions [9]. This spallation process will produce high energy photons, which will subsequently interact with the materials. It is necessary to have a complete nuclear dataset of photonuclear reactions for all isotopes of these elements. The experimental measurements of the nuclear reaction cross-section are one of the important methods to complete the nuclear dataset. However, there are always limitations in the experimental

measurements due to non-availability of all the energies of incident particles and preparation of target which may be unstable. For complete nuclear data for several isotopes, nuclear modular codes such as TALYS – 1.6 and EMPIRE – 3.2.2 are available. Using these codes one can predict the cross sections for different nuclear reaction channels. These codes basically use some nuclear models, and on the basis of the nuclear reaction theory, evaluation of the nuclear reaction data is done. The theory involved in photonuclear reaction cross section evaluation is discussed in the next section of this chapter. Apart from this, the nuclear systematics and empirical formula provide alternative method for such isotopes, as it can efficiently predict the nuclear properties. Many authors have used this theoretical approach. Several systematics and empirical studies have already been made for the photonuclear reactions [10]. These empirical formulae reduce experimental efforts, as they are basically dependent on well-known nuclear properties. In the present work, a new empirical formula has been developed and tested with nuclear modular codes and experimental data for $Z \geq 60$. With the help of the present empirical formula, one can predict the cross section datasets for those isotopes where there is a complete lack of the experimental data.

3.2. Theory of Photo Neutron Production

The known photon interactions are photoelectric effect, Compton scattering, and pair production. These interactions are the result of the interaction of a photon with atomic electrons. As the photon energy increases above 6 – 7 MeV, the interaction occurs with the nucleus. The interaction of high energy photon with the nucleus can cause ejection of nucleon/s. This reaction is referred as a photonuclear reaction. Photon should have sufficient energy above the binding energy of the nucleus for nucleon emission. As the nuclear binding energies are above 6 MeV for most of the isotopes, the photon should have such threshold energy [11]. Depending on the energy of the photon, three basic mechanisms are observed for the photonuclear reactions [12]:

(a) Giant dipole resonance (GDR)
(b) Quasi-deuteron (QD)
(c) Intra-nuclear cascade

If a gamma photon is having energy below 30 MeV, then it follows GDR mechanism. In this process, the photon energy is transferred to the nucleus by the oscillating electrical field of the photon, which induces oscillations inside nucleus

among nucleons. The photoneutron production is more probable since proton ejection needs to overcome a large Coulomb barrier. For different isotopes at a particular energy, there is a peak of photoneutron production for (γ, n) reaction. This energy is called GDR peak energy. For isotopes above Z = 60, the peak energies are between 10-18 MeV. Above 30 MeV, the photoneutron production is mainly due to the QD effect [12]. In this mechanism, a photon interacts with the dipole moment of a pair of proton-neutron in place of the nucleus as a whole [12]. Above 140 MeV, photoneutron production results from photo-pion production [12]. Further, the study of thermal fluctuation on GDR parameters is also of interest and studies are ongoing [13-16].

According to the semiclassical theory of the interaction of photons with nuclei, the shape of the fundamental resonance of the photoabsorption cross section follows a Lorentz curve [12, 17].

$$\sigma(E) = \frac{\sigma_i}{1 + [\frac{\left(E_\gamma^2 - E_m^2\right)^2}{E_\gamma^2 \gamma^2}]} \quad 3.1$$

Where, σ_i, E_γ and γ are the Lorentz parameters: peak cross section, resonance energy and full width at half maximum respectively [18].

In a more general way, in nuclear modular codes, such as TALYS – 1.6 and EMPIRE – 3.2.2, the photoabsorption cross section is calculated as the sum of two components [18-20],

$$\Sigma_{abs}(E_\gamma) = \sigma_{GDR}(E_\gamma) + \sigma_{QD}(E_\gamma) \quad 3.2$$

The component $\sigma_{GDR}(E_\gamma)$ represents the giant dipole resonance (GDR), in Lorentzian form. It is given by eq. 3.1 by as shown below,

$$\sigma(E) = \sum_i \frac{\sigma_i \cdot (E_\gamma \cdot \Gamma_i)^2}{\left(E_\gamma^2 - E_i^2\right)^2 + (E_\gamma \cdot \Gamma_i)^2} \quad 3.3$$

Where σ_i, E_i and Γ_i are: peak cross section, resonance energy and full width at half maximum respectively. The summation is limited to i=1 for spherical nuclei, while for deformed nuclei the resonance is split and one uses i = 1, 2. The component $\sigma_{QD}(E_\gamma)$, represents the Levinger form given by Chadwick et al. [19–22]. It is basically from the quasi-deuteron model. In the energy range from photonuclear threshold to 30 MeV, the GDR mechanism is dominant, while in the range 30 – 140

MeV QD mechanism is dominant. Above 140 MeV the threshold energy for pion production is achieved [21].

The above theory has been used in the TALYS – 1.6 and EMPIRE – 3.2.2 nuclear modular codes [23, 24]. Further details of these codes are given in literature [18–19]. Using these codes, (γ, n) nuclear reaction cross section for different isotopes ($Z \geq 60$) were calculated and are presented in the present thesis work. Until now, the photonuclear reaction cross sections have been evaluated using the Lorentz parameters. These parameters for several isotopes were calculated by fitting the experimental data or by systematics [25], but these parameters are not available for all the unstable isotopes.

3.3. Development of the Empirical Formula

3.3.1 Introduction

The present empirical formula has been developed using a few terms required to reproduce the cross section as a function of the incident photon energy. Initial derivation of the formula was done by using the earlier empirical formula used to explain neutron induced nuclear reaction cross section [26]. The present formula has three basic terms; 1. The fundamental term, 2. Isotopic resonance term and 3. Energy dependency term. These terms are discussed below.

3.3.2 Fundamental Term

In contrast to the Lorentzian parameters, the basic properties of nuclei A, N and Z were used to estimate the photonuclear cross section. Levovskii had given empirical formulae for (n, p) and (n, 2n) reaction cross section at 14.0 MeV [26],

$$\sigma(n, p) \propto \sigma_p \cdot e^{-\frac{33\cdot(N-Z)}{A}} \quad 3.4$$

$$\sigma(n, 2n) \propto \sigma_\alpha \cdot e^{-\frac{33\cdot(N-Z)}{A}} \quad 3.5$$

where $\sigma_p = \pi r_0^2 (A^{1/3} + 1)^2$ and $\sigma_\alpha = 0.4 \cdot \pi r_0^2 (A^{1/3} + 1)^2$

$r_0 = 1.2 \times 10^{-13}$ cm

These empirical formulae are based on A, N, and Z of a nucleus, and at fixed energy 14.0 MeV. These were modified to obtain an empirical formula for photo induced (γ,

n) nuclear reaction, which may be applied near to GDR peak energy. This modification is as given below.

$$\sigma(\gamma, n) \propto \sigma_m \cdot e^{-\frac{33.5\cdot(N-Z)}{A}} \quad 3.6$$

$$\sigma_m = \pi r_0^2 \cdot (A^{2/3} + 1)^2 \cdot (N - Z) \cdot A^{\frac{-4}{3}} \quad 3.7$$

where r_0 is the average nuclear radius. This is taken as the fundamental term of the present empirical formula.

3.3.3 Isotopic Resonance Term

The experimental data shows the resonance nature of the reaction cross section, which depends on the isotope, i.e., the GDR peak energy is different for the different isotopic number. Thus for a given GDR peak, the cross section decrement is distributed on the either sides of GDR peak energy. Hence a term representing such phenomena must be included.

The modified formula is given below,

$$\sigma(\gamma, n) \propto \sigma_m \cdot e^{-\frac{33.5\cdot(N-Z)}{A}} \cdot e^{\left(-\left(\frac{\left(Ei - S_j \cdot R_p\right)}{2}\right)^2\right)} \quad 3.8$$

Where E_i and R_p are the incident photon energy and resonance parameter respectively.

In this modification, two parameters are specifically used, R_p and S_j.

The parameter S_j can be calculated by,

$$S_j = \frac{A^2}{2(N-Z)^2} \quad 3.9$$

The parameter R_p is estimated for an isotope, by fitting the (γ, n) nuclear reaction cross section using the above formula for different isotopes of the same element. It was observed that this parameter R_p is following a linear relationship against the atomic mass of the different isotopes of the same element, which can be written in the form of the following equation,

$$R_p = m \cdot A + C \quad 3.10$$

Where A is the atomic mass of the isotope, and m and C are the slope and intercept respectively, More details of this parameter (R_p) for different elements is given in subsection 3.3.5.

This term $e^{-[\{\frac{(Ei-S_j \cdot Rp)}{2}\}^2]}$ depends on the energy of the incident photon and the isotopic nature of the target nucleus. When a photon is incident on the nucleus, the response depends on the photon energy. If the incident photon is below the threshold energy for photo fission, it cannot eject a nucleon from the nucleus. If energy of the photon is above the threshold energy of the (γ, n) reaction, the reaction cross section increases until the resonance peak energy is reached. After this energy, again the cross section decreases. This is incorporated using this exponential term. The subtraction of $S_j \cdot R_p$ from the incident photon energy shows the isotopic dependence of the resonance peak energy of the reaction. It was observed in the experimental data that as the isotopic number increases, the GDR peak shifts towards the lower energy side. This back shift effect can be calculated with the exponential term considered here. The value of $S_j \cdot R_p$ increases with addition of neutrons to the isotope nucleus. This means that when a photon is incident on the target isotope, it interacts with the last shell neutron in the nucleus. The binding energy of the last added neutron will be least. Hence the photon may require smaller energy to initiate the resonance isotope number.

This phenomenon can be observed in FIGS 3.1 and 3.2, showing the isotopic effect for the resonance peak energy back shifting in Nd and Pt isotopes using the above exponential term.

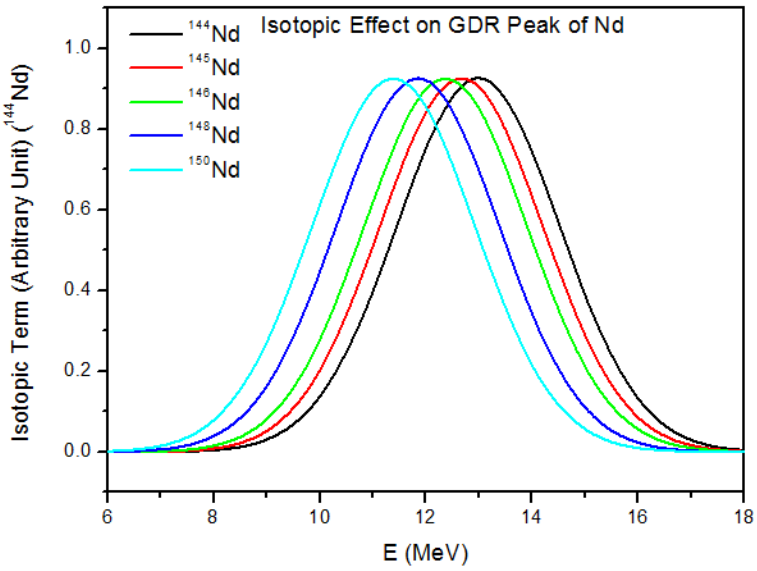

FIG 3.1 Backshift of Resonance Peak Energy in Nd isotopes which is result from the term $e^{\left(-(\frac{(Ei-Sj \cdot Rp)}{2})^2\right)}$

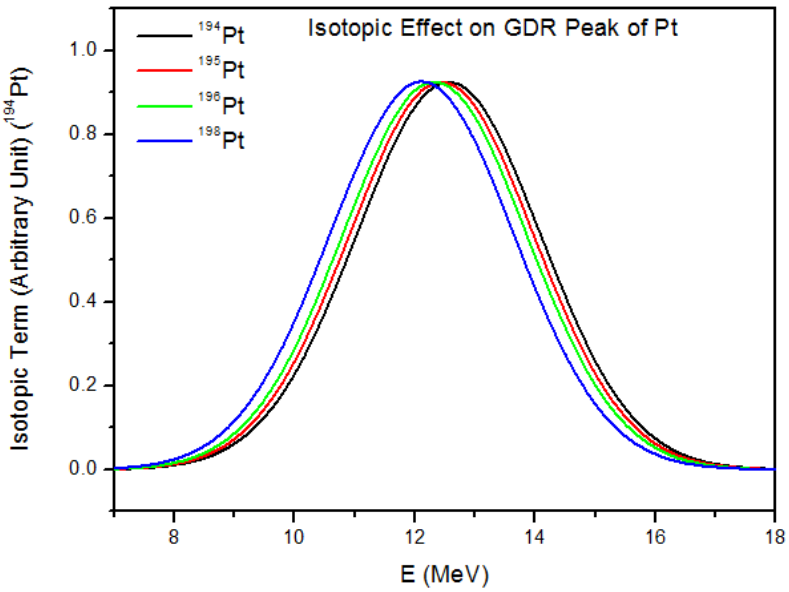

FIG 3.2 Backshift of Resonance Peak Energy in Pt isotopes which is result from the term $e^{\left(-(\frac{(Ei-Sj\cdot Rp)}{2})^2\right)}$

3.3.4 Energy Dependency Term

There is a need to introduce an energy related term to make the formula to predict the cross section more accurately. If the photon energy increases, then it can transfer more energy to the nucleus. In the mechanism of GDR, the oscillating electrical field transfers its energy to the nucleus by inducing an oscillation in the nucleus, which leads to the relative displacement of tightly bound neutrons and protons inside the nucleus [12]. When the energy of the photon is low (near to the threshold), the oscillating electric field of the photon interacts with the collective nuclear field produced by the sum effect of all the nucleons. However, as the energy of the photon increases, the oscillating electrical field interacts with a pair of neutron and proton rather than the whole nucleus. This can be accounted by the term $e^{\sqrt{1+E^{\frac{2}{3}}}}$, where E is the energy of the incident photon. This term shows that photon can have more energy to transfer to the nucleons as the incident photon energy increases. It also indicates that as the energy of the photon increases, it can have less interaction time with nucleons. In this way, the emission of neutrons by pre-equilibrium or direct reaction mechanism can also be explained.

Hence, by the addition of an energy dependent term, the modified formula becomes,

$$\sigma(\gamma, n) \propto \sigma_m \cdot e^{-\frac{33.5\cdot(N-Z)}{A}} \cdot e^{\left(-\left(\frac{\left(Ei-S_j\cdot Rp\right)}{2}\right)^2\right)} \cdot e^{\sqrt{1+E^{\frac{2}{3}}}} \qquad 3.11$$

An additional factor S_f which depends on isospin has been introduced to complete the formula. This factor was plotted and fitted for different isotopes of the same element. It was observed that factor follows some exponential relation, which is described in subsection 3.3.6. This empirical formula gives the cross section to the order of milli-barn.

The final modified formula is now given below,

$$\sigma(\gamma, n) = \sigma_m \cdot e^{-\frac{33.5\cdot(N-Z)}{A}} \cdot e^{\left(-\left(\frac{(Ei-Sj\cdot Rp)}{2}\right)^2\right)} \cdot e^{\sqrt{1+E^{\frac{2}{3}}}} \cdot S_f \qquad 3.12$$

3.3.5 R_p Parameter

As discussed in section 3.3.3, the parameter R_p is used to show the isotope dependency of the reaction cross section. In the empirical formula the term $e^{-[\{\frac{(E_i-S_j\cdot R_p)}{2}\}^2]}$, contains the S_j and R_p parameters. The parameter R_p is responsible for the change in the cross section due to atomic number, where the product of S_j and R_p accounts for the isotopic back shift effect, as shown in FIGS. 3.1 and 3.2. The parameter R_p for different isotopes can be calculated using a linear relation given by eq. 3.10 with the atomic mass number of isotopes for an element. Therefore, the plots of R_p against A for different elements should be parallel lines with different intercepts on R_p axis as shown in FIG 3.2. It is a property of parallel lines that they have same slope but different intercepts. Hence, the mean slope of the different element has been taken as the standard slope for all elements ($Z \geq 60$). This value of the slope (m) mentioned in eq. (10) is ~ 0.03164 ± 0.00409. The intercept C for different elements are plotted against the atomic number of an element, and fitted with mathematical software MATLAB, using 3rd degree polynomial as shown in FIG 3.3. The intercept C for a different element can be determined from the following equation.

$$C(Z) = p_1\cdot Z^3 + p_2\cdot Z^2 + p_3\cdot Z + p_4 \qquad 3.13$$

with $p_1 = -4.155 \times 10^{-5}$, $p_2 = 0.008971$, $p_3 = -0.7156$, and $p_4 = 15.78$, Z = Atomic number

(SSE: 0.00147; R-square: 0.9998: Adjusted R-square: 0.9996; RMSE: 0.01917)

Hence, the intercept for any element can be evaluated using the above eq. 3.13, which is fixed for different isotopes of the same element. Using this intercept and the slope 0.03164 ± 0.00409 one can calculate the parameter R_p from eq. 3.10. The model values of the parameter R_p for different elements are compared with the previous manually selected values as shown in FIG 3.2.

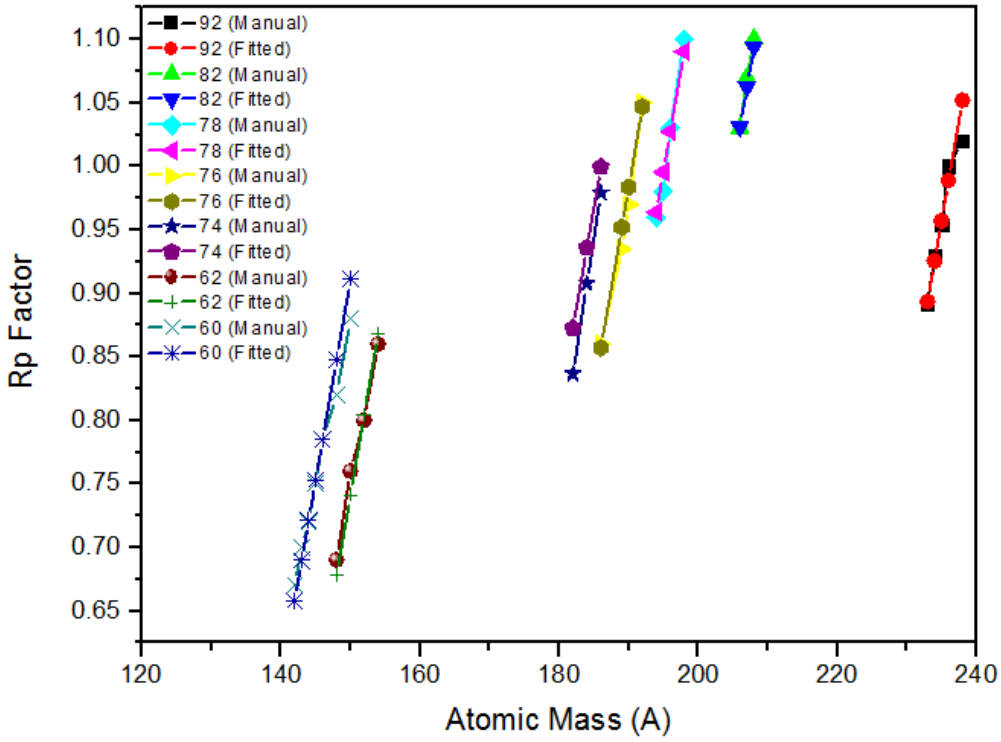

F IG 3.3 R_p parameter fitted for different elements using eq. 3.10

3.3.6 S_f Parameter

This parameter includes the isospin effect, as discussed by J. S. Wang *et al*., [27]. In order to include this effect in the empirical formula, an additional factor called S_f has been added. This factor was initially added and then, in order to generalize it is fitted with different combinations of N, Z and A. Thus it follows a complex exponential relation with exp((N – Z)/N) of an isotope. This parameter S_f is also considered as a result of the asymmetry of the nucleus. As there is a difference in neutron and proton number, the fraction (N – Z)/N is the available neutron fraction for a photon to eject. As this fraction value increases, the value of S_f also increases, which directly shows increment in the photoabsorption cross section of that isotope.

This isotopic factor S_f for different isotopes is plotted with respect to exp((N – Z)/N,) and fitted with MATLAB software as shown in FIG 3.4. The generalized expression to determine S_f parameter for an isotope is as given below.

$$S_f = ae^{bx} + ce^{dx} \qquad 3.14$$

where, x = (N – Z)/N, a = 1.21×10^{-22}, b = 34.21, c = 7.71×10^{-11}, d = 14.52

(SSE: 0.006977; R-square: 0.9781; Adjusted R-square: 0.9759; RMSE: 0.01551)

Looking at FIG 3.5 carefully, when $e^{\frac{(N-Z)}{N}}$ is between 1.40 to 1.42, then S_f factor has almost same values. These S_f values are for Z = 82 and N = 124, 125, 126, which is either a magic number or near to the magic number. S_f is purely dependent on (N – Z)/N, which is a shell dependent term. The anomalous behavior of the S_f factor values for these isotopes is due to the magic shell effect.

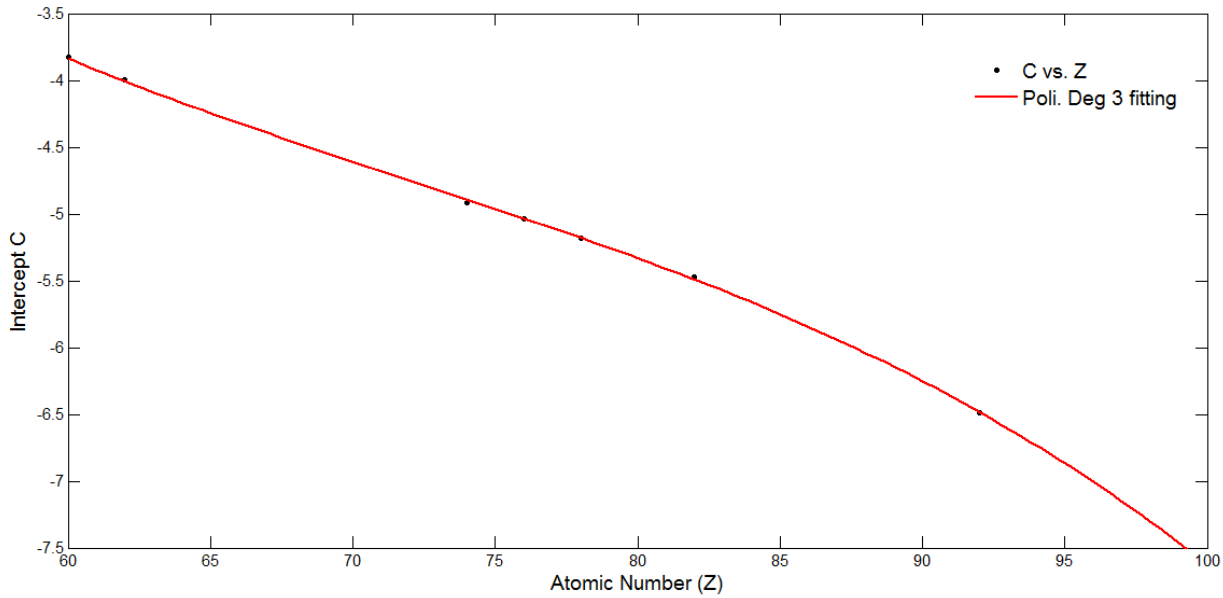

FIG 3.4 Intercept C for eq. 3.10 for different elements fitted with eq. 3.11

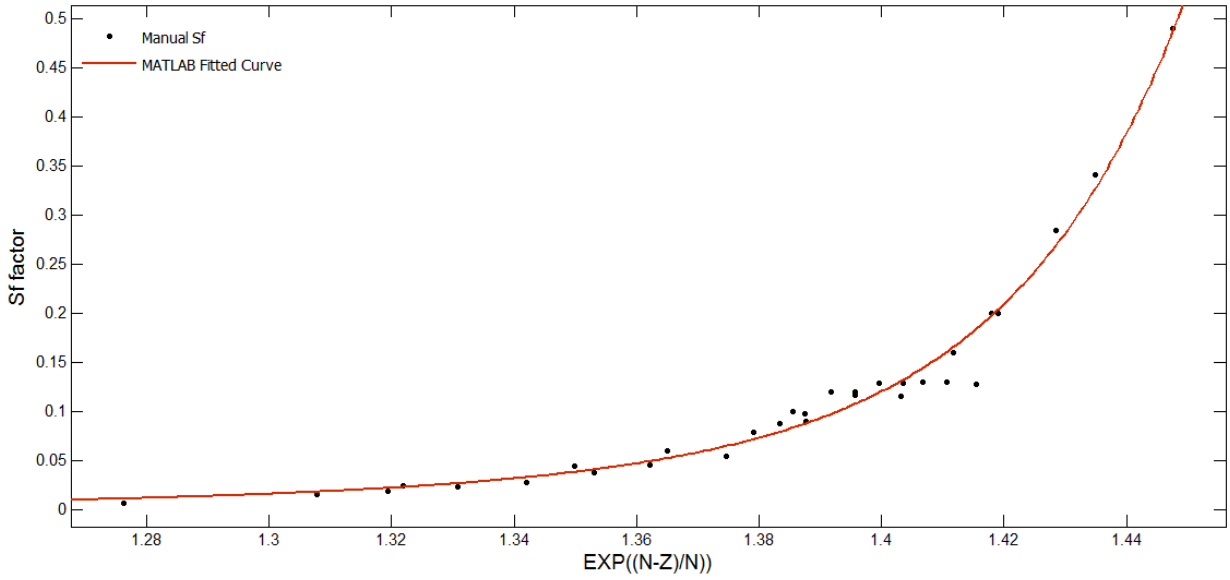

FIG 3.5 S_f parameter for different (N-Z)/N fitted with eq. 3.14

3.4. Results and discussion

The (γ, n) reaction cross section for different isotopes with Z ≥ 60 was calculated using the newly developed empirical formula. In addition, the nuclear modular codes TALYS – 1.6 and EMPIRE – 3.2.2 were also used to predict the same cross section in order to compare the predictability of present empirical formula and Lorentz curve based model. All the results are compared with the available EXFOR data [28] and are shown in FIGS. 3.6 – 3.10. The cross sections are calculated for the energy range near to GDR peak. The results obtained by modular codes and empirical formulae are in agreement with the experimental data as shown in FIGS. 3.6 – 3.10. However, the empirical formula is giving more appropriate cross section results and predicts the nuclei behavior near to the GDR peak energy region. This empirical formula is good for those isotopes which have a single GDR peak. In most of the cases studied here, that have a single GDR peak, the empirical formula gives good agreement near to the GDR peak energy as compared to the model based on Lorentz curve fitting.

In the case of the isotopes with Z from 63 to 75, it was found that collective model predicts large nuclear quadrupole moment. The quadrupole moment exists because of the asymmetry of the nucleus. The nuclei are found in the middle of the 1d, 2s shells in the range of 145 < A <185. The energy difference between the ground state and the first excited state is of the order of hundreds of keV. In the deformed nucleus, the incident photon can interact either with the ground state or with the excited state

nucleons and hence can produce a resonance at two different nearby energies. This is observed in the above isotopes. For such cases, the Lorentz curve based model, viz. TALYS – 1.6 and EMPIRE – 3.2.2, works reliably for these isotopes, as shown in FIG 3.11. For some cases, however, the TALYS – 1.6 and EMPIRE – 3.2.2 model does not work well, e.g. FIG 3.11(e – f). In order to apply the empirical formula for such isotopes, it is assumed that there may be two peaks due to unresolved resonances occurring near the energies of ground and excited nuclei, which are due to the quadrupole moment. This suggests parameters R_p and S_f can have two different values for these isotopes. It indicates that the energy dependence cross section curve is made of two curves with two different R_p (R_{p1} and R_{p2}) and S_f values (S_{f1} and S_{f2}) of parameters R_p and S_f respectively. These values can be estimated by multiplying the following factors to the R_p and S_f values calculated from Sections 3.3.5 and 3.3.6.

$$R_{p1} = 0.95 \text{ x } R_p \tag{3.15}$$

$$R_{p2} = 1.20 \text{ x } R_{p1} \tag{3.16}$$

$$S_{f1} = 1.39 \text{ x } S_f \tag{3.17}$$

$$S_{f2} = 0.28 \text{ x } S_{f1} \tag{3.18}$$

The two curves are intersecting at a deep point, where both curves should have the same value of cross section. This intersection point energy can be calculated by comparing the right side of the eq. 3.12 for above values.

$$\sigma_m \cdot e^{-\frac{33.5\cdot(N-Z)}{A}} \cdot e^{\left(-\left(\frac{(Ei-S_j\cdot R_{p1})}{2}\right)^2\right)} \cdot e^{\sqrt{1+E^{\frac{2}{3}}}} \cdot Sf1 = \sigma_m \cdot e^{-\frac{33.5\cdot(N-Z)}{A}} \cdot e^{\left(-\left(\frac{(Ei-S_j\cdot R_{p2})}{2}\right)^2\right)} \cdot e^{\sqrt{1+E^{\frac{2}{3}}}} \cdot Sf2 \tag{3.19}$$

Solving this eq. we get,

$$E_{deep} = \frac{1}{2} S_j \cdot (R_{p1} + R_{p2}) + \frac{2 \ln\left(\frac{S_{f2}}{S_{f1}}\right)}{S_j (R_{p1} - R_{p2})} \tag{3.20}$$

This energy E_{deep} is near to the threshold energy of the (γ, 2n) reaction. With this consideration, the results are plotted in FIG 3.11(a – f).

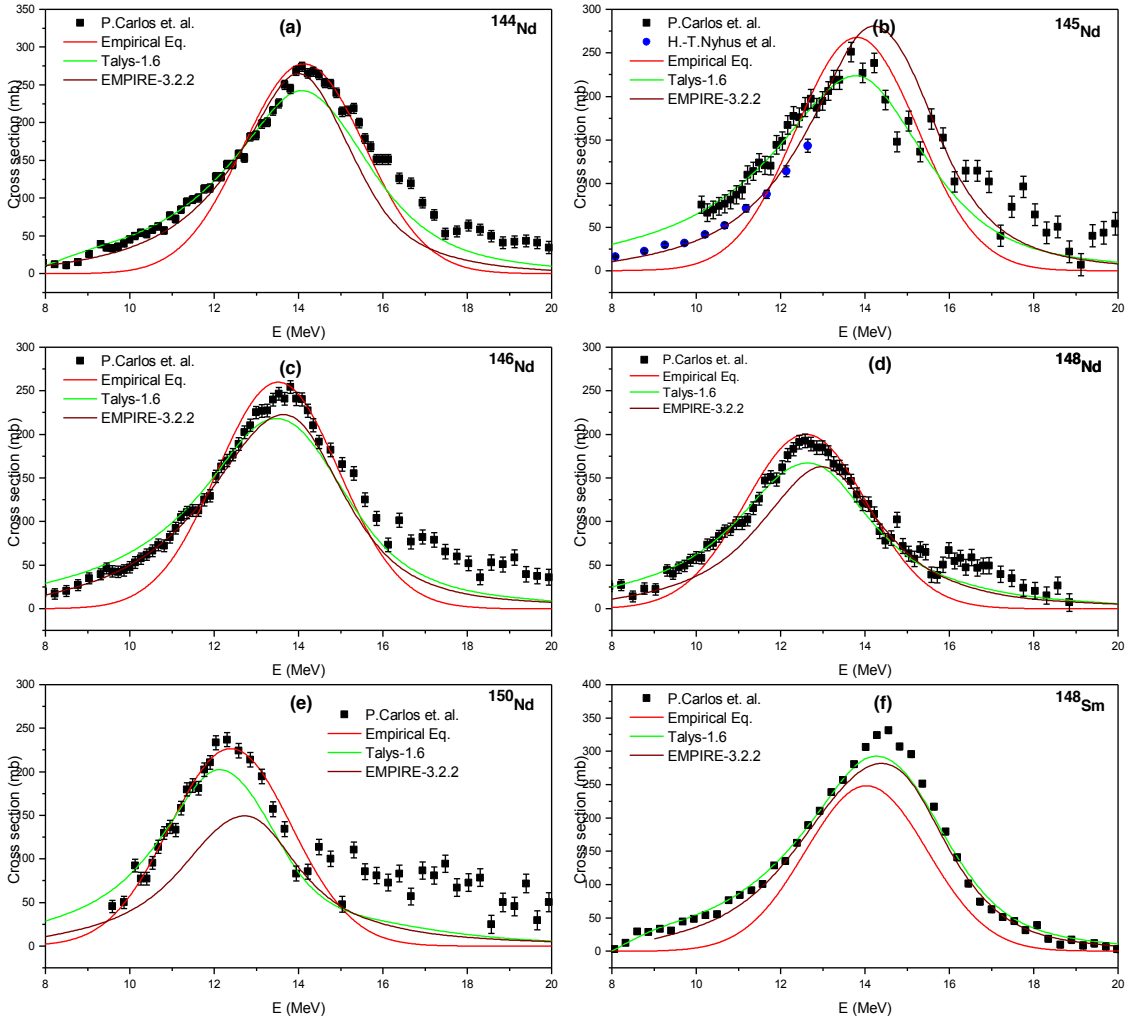

FIG 3.6 Comparison of Evaluated data using TALYS-1.6, EMPIRE-3.2.2, and Empirical Formula with Experimental data from EXFOR comparison for $^{144\text{-}146,148,150}$Nd, and ^{148}Sm

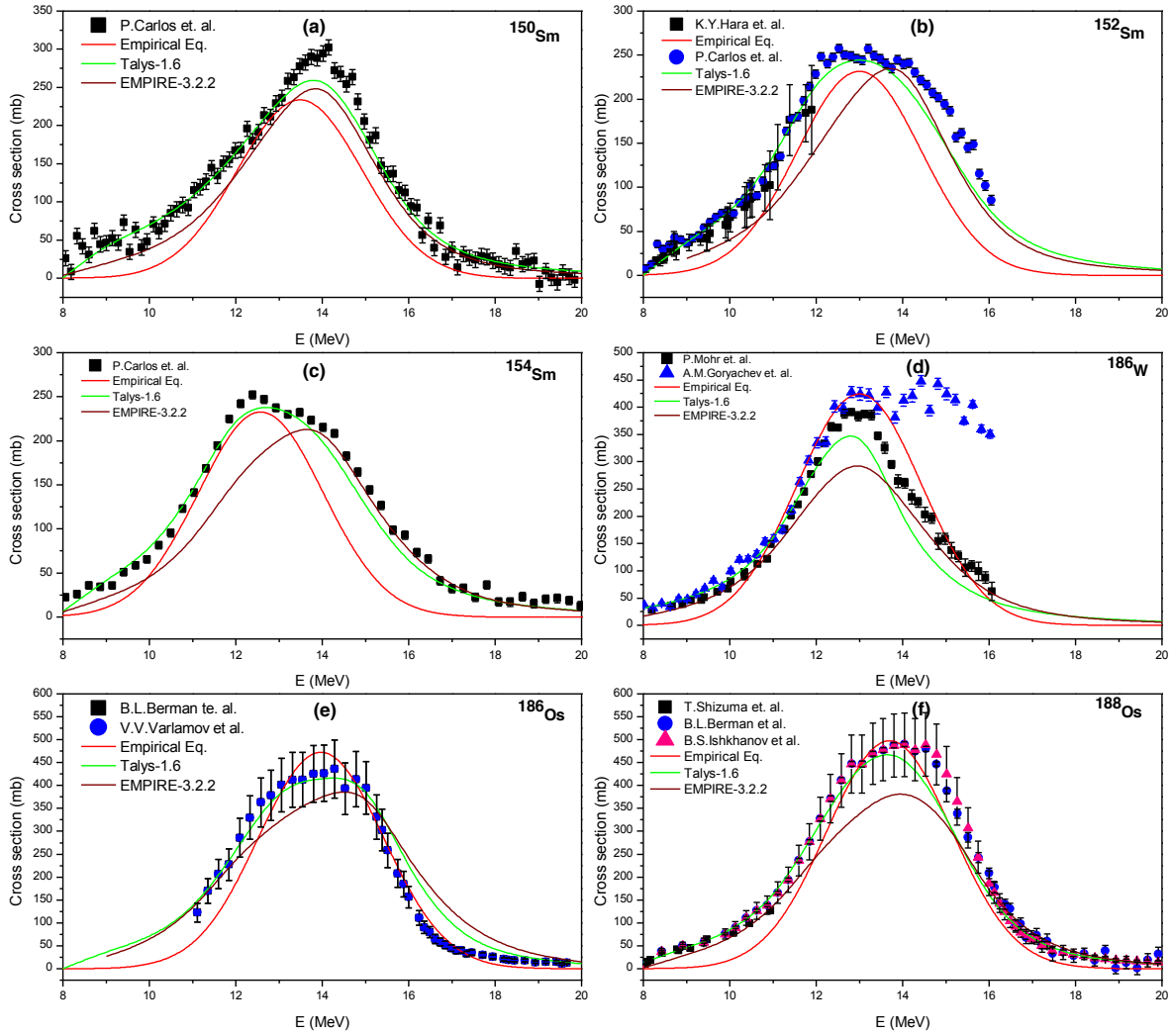

FIG 3.7 Comparison of Evaluated data using TALYS-1.6, EMPIRE-3.2.2, and Empirical Formula with Experimental data from EXFOR comparison for ^{150,152,154}Sm, ^{186}W, ^{186}Os, and ^{188}Os

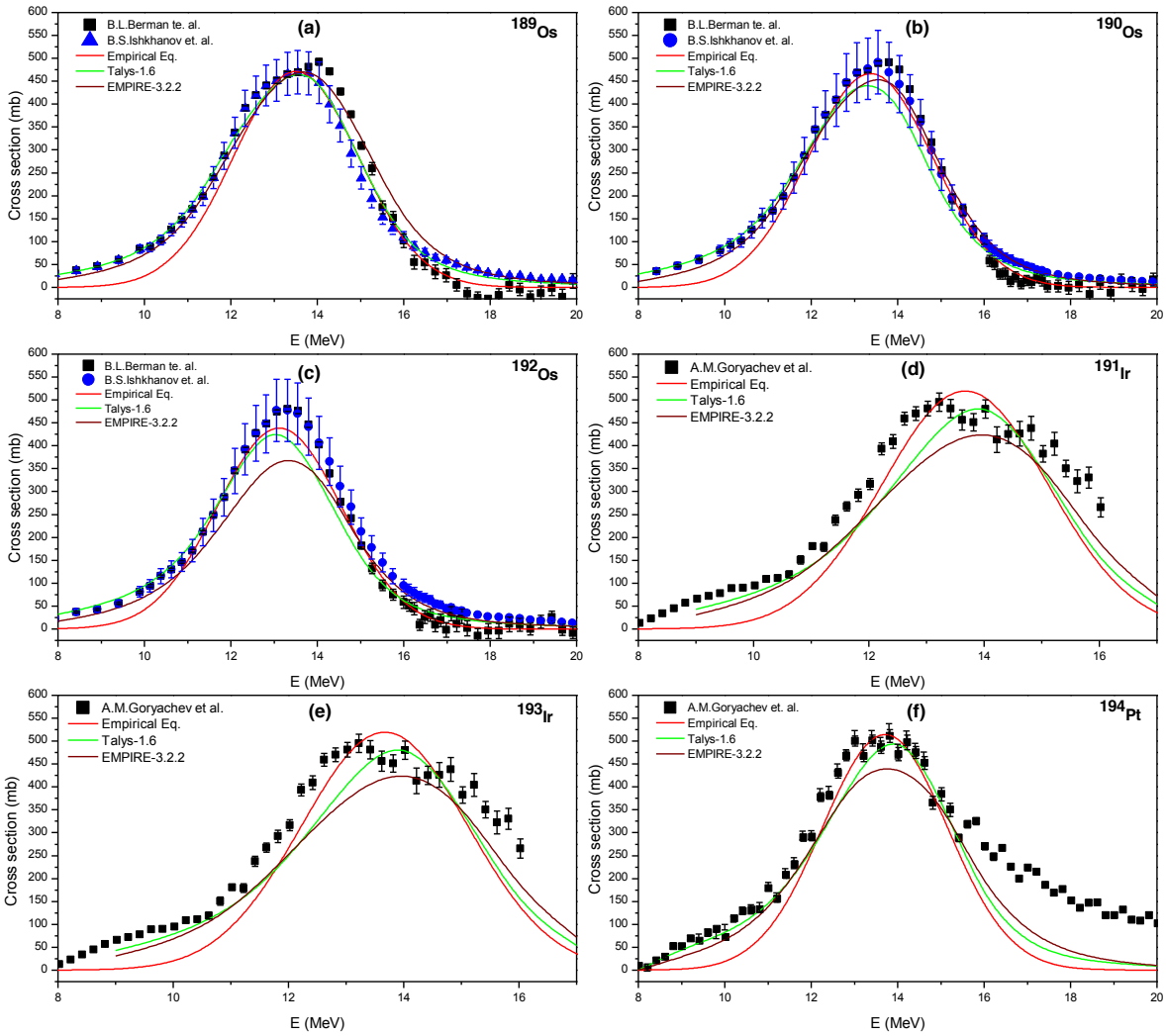

FIG 3.8 Comparison of Evaluated data using TALYS-1.6, EMPIRE-3.2.2, and Empirical Formula with Experimental data from EXFOR comparison for $^{189\text{-}190,192}$Os, ^{191,193}Ir, and ^{194}Pt

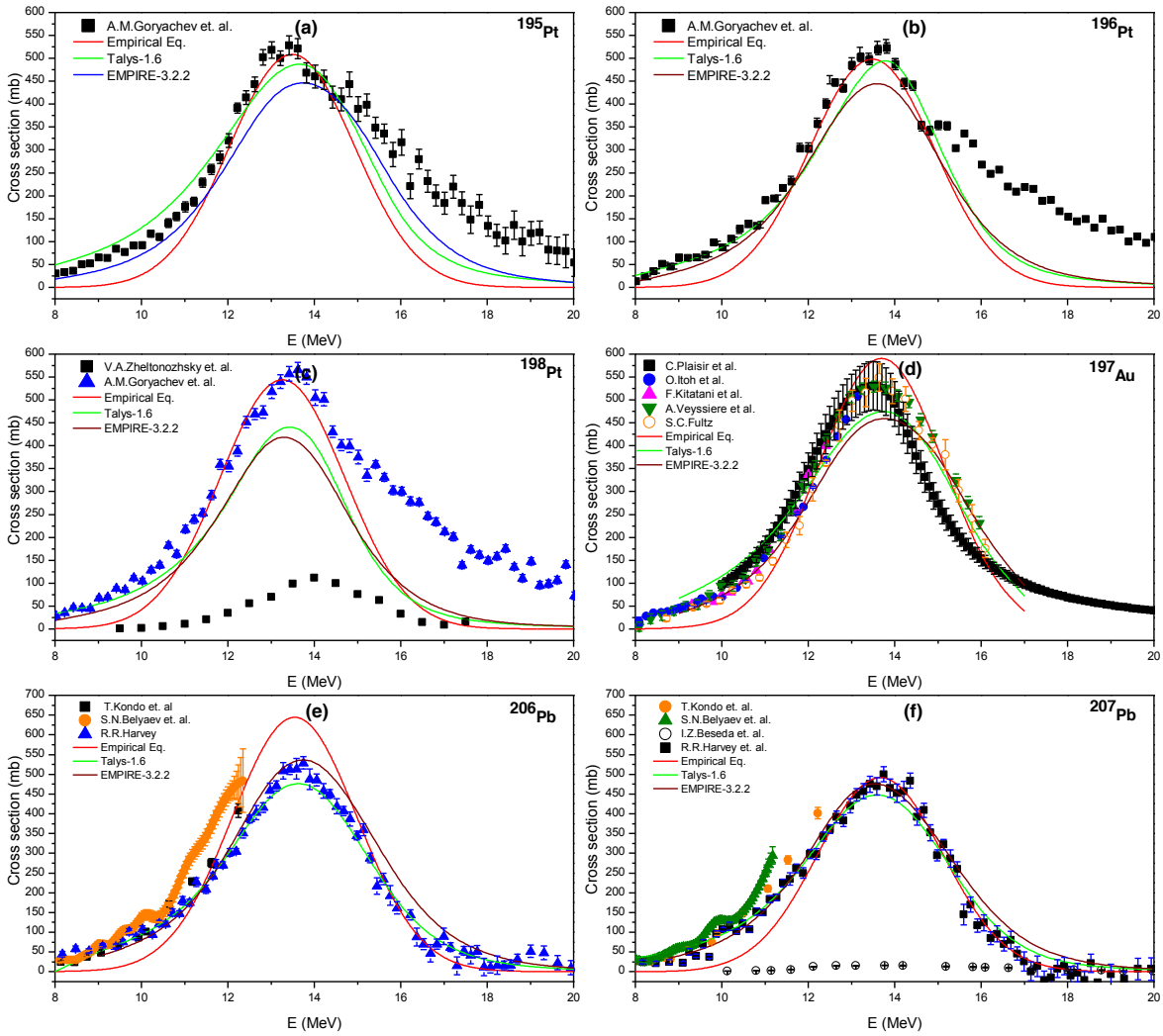

FIG 3.9 Comparison of Evaluated data using TALYS-1.6, EMPIRE-3.2.2, and Empirical Formula with Experimental data from EXFOR comparison for $^{195\text{-}196,198}$Pt, ^{197}Au, ^{206}Pb, and ^{207}Pb

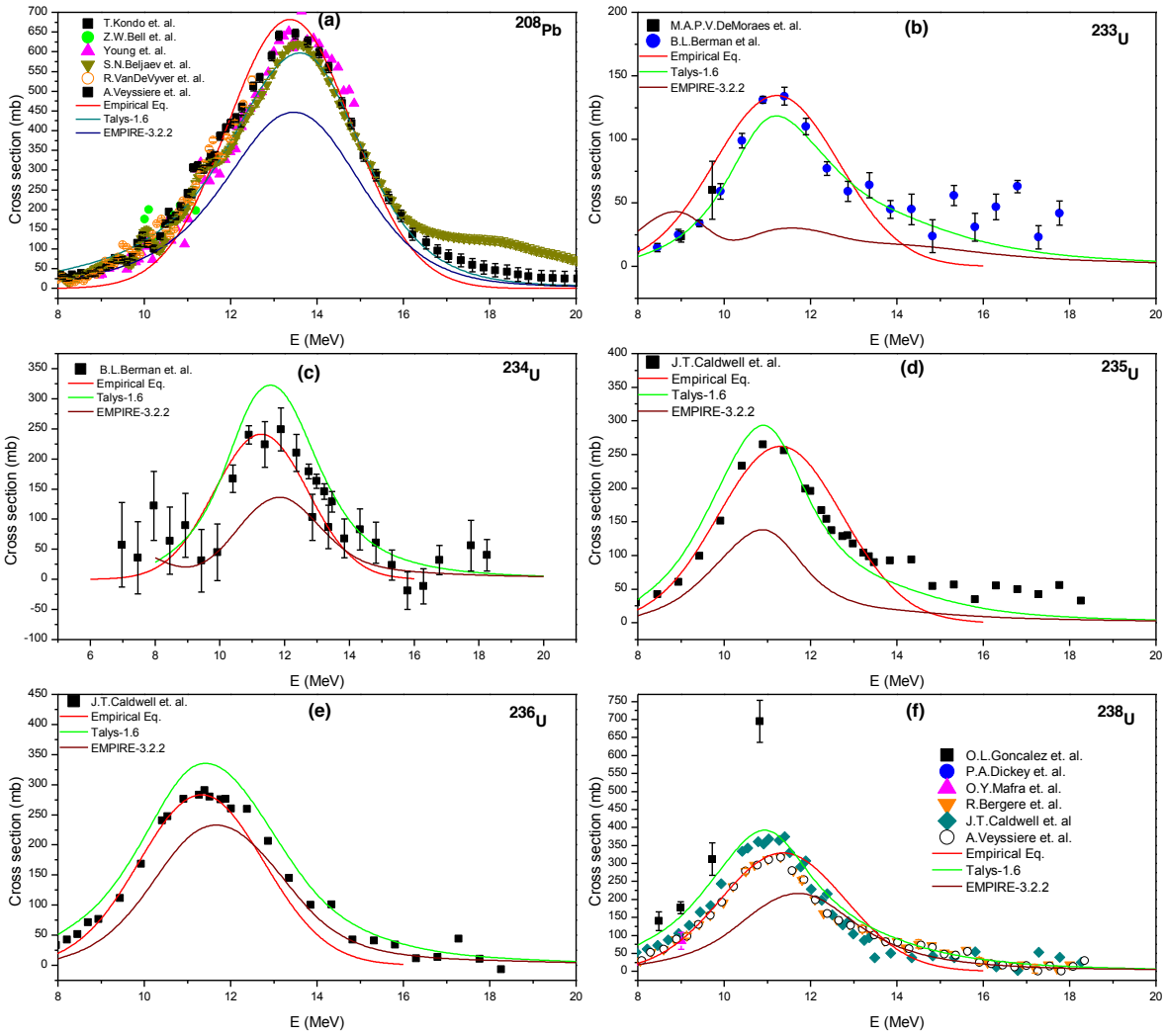

FIG 3.10 Comparison of Evaluated data using TALYS-1.6, EMPIRE-3.2.2, and Empirical Formula with Experimental data from EXFOR comparison for ^{208}Pb, $^{233-236}$U, and ^{238}U

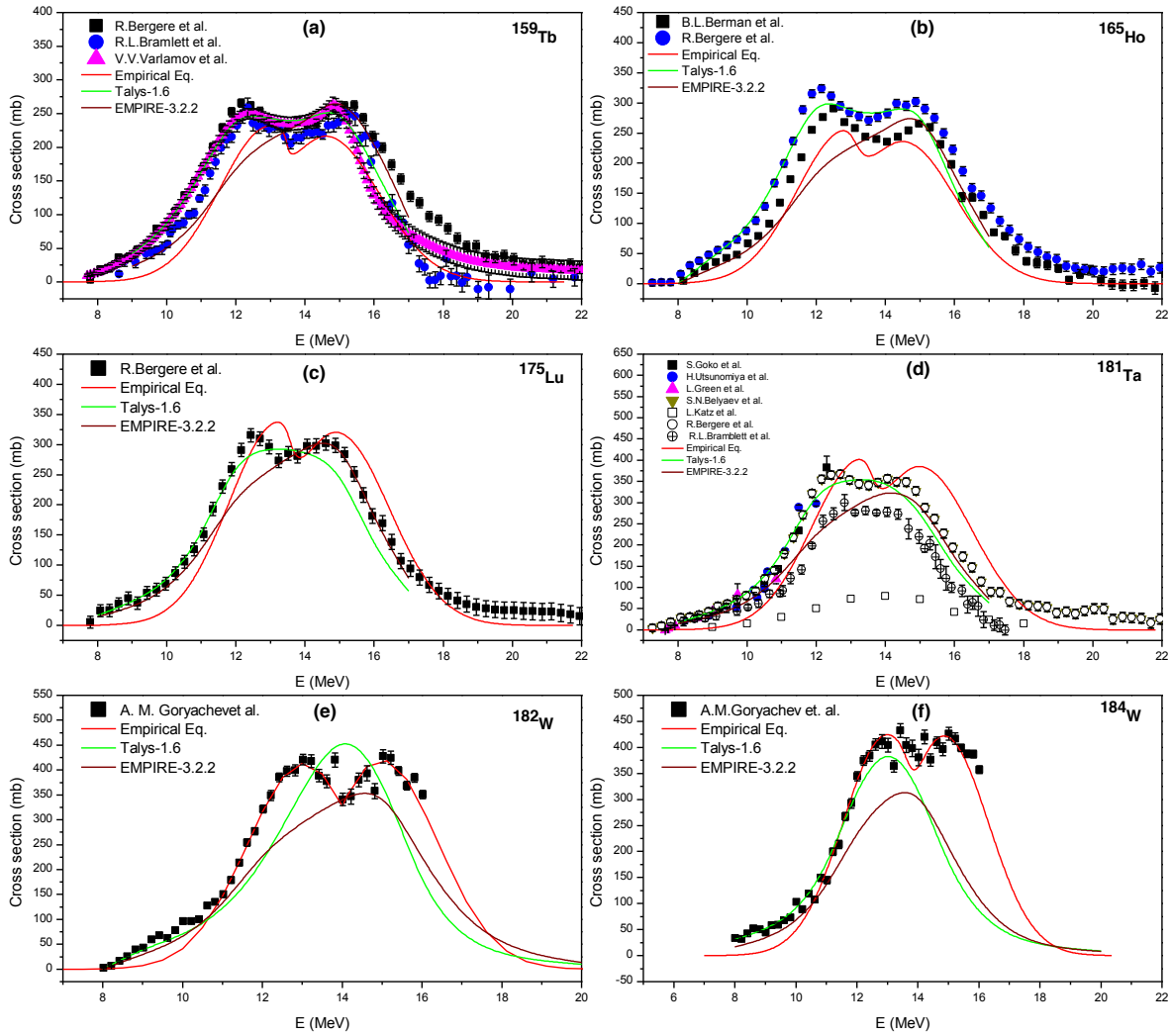

FIG 3.11 Effect of deformed nuclei in (γ, n) nuclear reaction, data comparisons for TALYS – 1.6, EMPIRE – 3.2.2 and Present Empirical formula

3.5. Applications of the Present Empirical Formula

The present empirical formula can be used to predict cross section for (γ, n) reaction for the isotopes with $Z \geq 60$. Here cross section of some selected (γ, n) reaction for some selected reactions was calculated and presented. The (γ, n) cross section for several isotopes of W, Pb, Pa, U and Pu, which have no available experimental data, were calculated using present empirical formula and compared with TALYS – 1.6, EMPIRE – 3.2.2 evaluated data.. Further, the predicted data of the isotopes were compared with different standard evaluated data libraries, wherever available.

Tungsten is a prime candidate for the plasma facing component in a fusion reactor. It is selected for the diverter material in the ITER fusion reactor [4]. Tungsten isotopes

^{182}W, ^{184}W and ^{186}W have experimental data for the (γ, n) reaction cross section [28]. The (γ, n) cross section for remaining isotopes ^{180}W(0.12%) and ^{183}W(14.31%) were calculated and compared with the evaluated data available in ENDF/B-VII.1. No other standard data library has photonuclear data for these tungsten isotopes [19]. There is an agreement between present evaluated data and ENDF/B-VII.1 as can be seen in FIG 3.12 (a – b), where there is not good agreement in FIG 3.13 (c – d). Lead is a prime element for the Pb-Li blanket module of the fusion reactors, as well as, it is also a candidate for the ADS target material [29]. Experimental data are available for lead isotopes ^{206}Pb, ^{207}Pb and ^{208}Pb. The (γ, n) cross section for remaining isotopes of lead ^{202}Pb (5.25×10^4 y, [30]), ^{203}Pb (51.92 h, [30]), ^{204}Pb (1.4×10^{17} y, [30]) and ^{205}Pb (1.73×10^7 y, [30]) were calculated and presented. These isotopes of lead have a large half-life and they are facing high energetic photons during the runaway electron generation and the disruption phase in plasma [5]. There are some isotopes of Pa and U: ^{231}Pa(3.27×10^4 y, [30]), ^{232}U(68.9 y, [30]) and ^{237}U(6.75 d, [30]) having no evaluated cross section data in various standard data libraries, such as ENDF/B-VII.1, JENDL-4.0, JEFF-3.1, ROSFOND and CENDL-3.1 [31,32]. The cross sections for these isotopes were also calculated and presented. The evaluated data for ^{239}Pu (2.41×10^4 y, [30]) and available data in ENDFB/VII.1 are presented in FIG 3.13 (d). Though in the present context, cross sections are evaluated for limited isotopes, it can be applied to calculate (γ, n) reaction cross section for actinides using the nuclear modular codes and present empirical formula. While the TALYS – 1.6 and EMPIRE – 3.2.2 codes can be used to calculate the (γ, n) reaction cross section for the isotopes, which have available GDR parameters, whereas the present empirical formula can be used to calculate cross section for any isotope with $Z \geq 60$.

Another important application is, to use the nuclear modular codes and the present formula to calculate the incident gamma energy for which, the cross section will have maximum value i.e. at the GDR peak energy. It can be used to calculate the incident charge particle (e.g. electron) beam energy for the bremsstrahlung production, which is required to design a photoneutron source. There are some theoretical transport codes available to transport the electrons and photons such as MCNP [12, 33-34], FLUKA [35, 36], GEANT [37] etc. Using these codes, one can estimate the bremsstrahlung spectra from the electron beam.

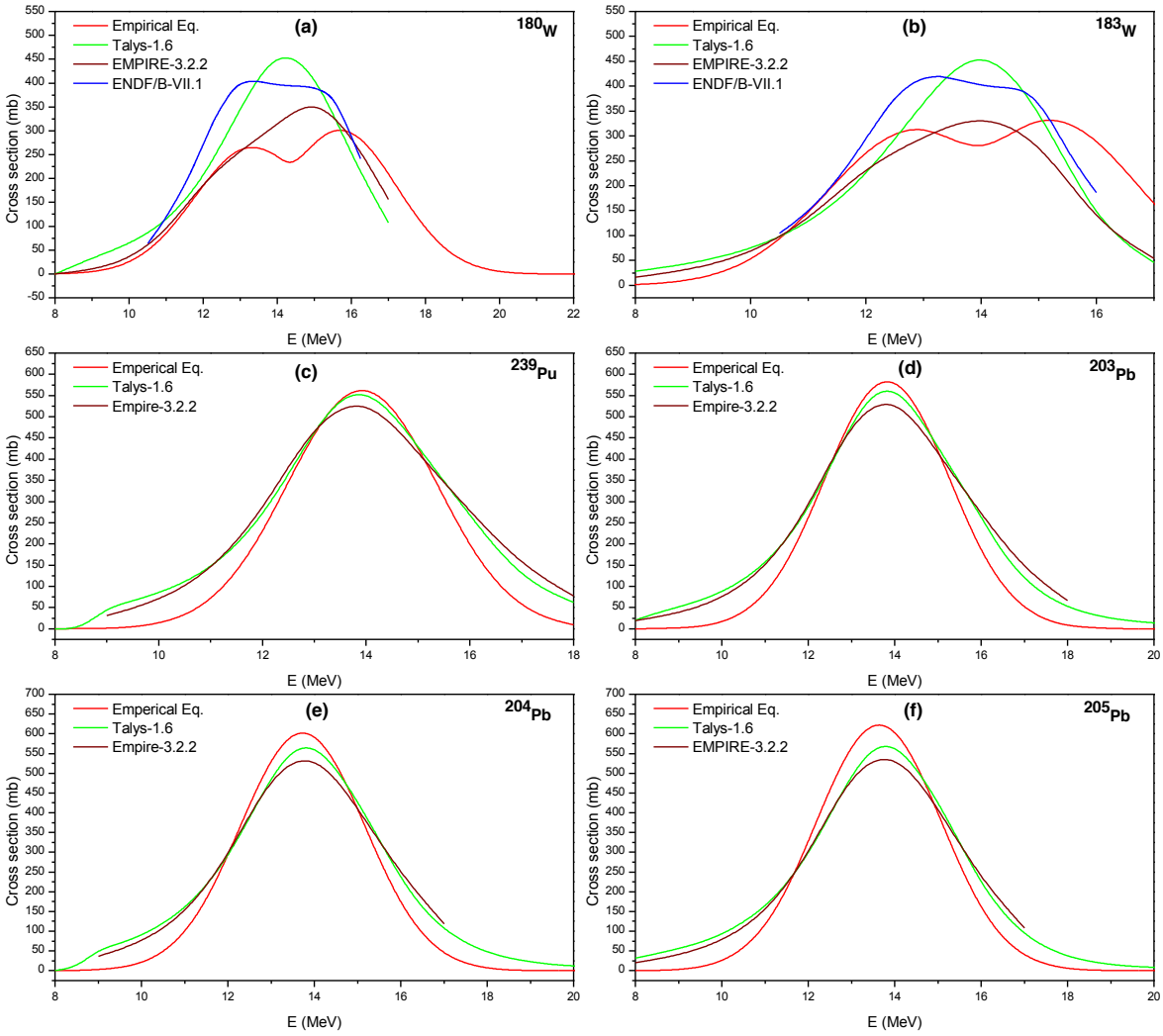

FIG 3.12 Comparison of Evaluated data for ^{180,183}W, $^{202\text{-}204}$Pb, and ^{205}Pb using TALYS -1.6, EMPIRE-3.2.2, and empirical formula

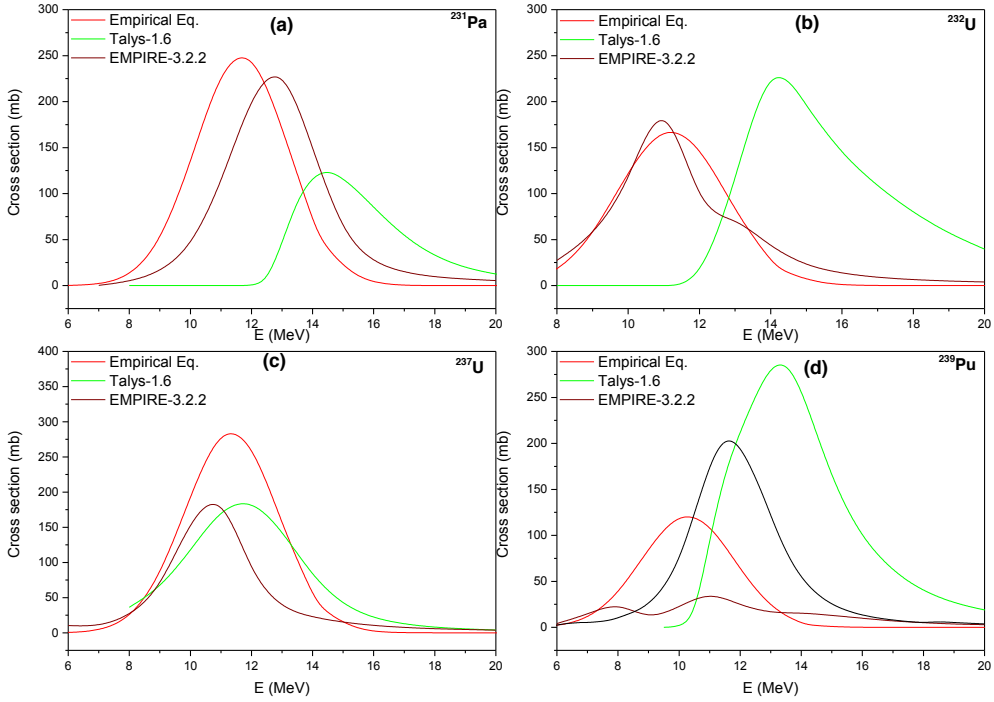

FIG 3.13 Comparison of Evaluated data for ^{231}Pa, ^{232,237}U, and ^{239}Pu using TALYS - 1.6, EMPIRE-3.2.2, and Empirical Formula

3.6. Summary and conclusions

A new empirical formula has been developed to investigate the (γ, n) reaction cross section for isotopes with Z ≥ 60 in the GDR energy region. The results for the (γ, n) reaction cross section obtained by using the above empirical formula has been reproduced by using the nuclear modular codes: TALYS – 1.6 and EMPIRE – 3.2.2. It has been shown that TALYS – 1.6, EMPIRE – 3.2.2 and the empirical formula is in agreement with the experimental data. Further, a conclusion may be drawn that there may be no deformation in the GDR peak of a pure (γ, n) reaction cross section for the spherical nucleus. As a result of the quadrupole moment, which is due to the asymmetric shape of the nucleus, the present deformation has been observed.

In addition to this, the evaluated data for $^{180\text{-}184}$W, $^{202\text{-}205}$Pb, ^{231}Pa, $^{232\text{-}237}$U, and ^{239}Pu using TALYS – 1.6, EMPIRE – 3.2.2 and our empirical formula have been presented. Among these only ^{180}W, ^{183}W and ^{239}Pu have evaluated data in ENDF/B-VII.1 [29], which are compared with the present evaluated data. For $^{180\text{-}184}$W, the present evaluated data are in good agreement, but in the case of ^{239}Pu, it is in disagreement. It is necessary to do experiments in the GDR energy range to validate the present

evaluated data for ^{239}Pu. Further, though here only limited isotopes have been used for the (γ, n) reaction cross section evaluation, the empirical formula can be applicable to other isotopes provided $Z \geq 60$.

References

[1] http://www-pub.iaea.org/MTCD/publications/PDF/te_1178_prn.pdf, retrieved 16th May 2016

[2] A.R. Junghans, et al., Phys. Lett. B, 670: 200 (2008)

[3] S. J. Zweben, H. Knoepfel, Phys. Rev. Lett., 35: 1340 (1975)

[4] R. A. Pitts, et al., Journal of Nuclear Materials, 463: 39-48 (2013)

[5] A. Shevelev, et al., doi: 10.1063/1.4894038, retrieved 17th May 2016

[6] B. L. Berman, et al., Phys. Rev., 162: 1098 (1967)

[7] C. H. M. Broeders, et al., Nucl. Eng. Des., 202: 157 (2000)

[8] F. R. Allum, et al., Nucl. Phys. A, 53 645 (1964)

[9] H. Naik, et al., Nucl. Phys. A, 916: 168-182 (2013)

[10] I. Raškinyte˙, et al., in Proc. Int. Conf. on Nuclear Reaction Mechanisms, (Varenna, Italy: Dapnia/SPhN, 2006), DAPNIA-06-147

[11] G. Kim, et al., Nucl. Instrum. Methods Phys. Res., Sect. A, 485: 458-467 (2002)

[12] V. C. Petwal, et al., PRAMANA — journal of physics, 68: 235 (2007)

[13] M. Gallardo, et al., Phys. Lett. B, 191: 222-226 (1987)

[14] M. Mattiuzzi, et al., Phys. Lett. B, 364: 13-18 (1995)

[15] P. Heckman, et al., Phys. Lett. B, 555: 43 (2003)

[16] Balaram Dey, et al., Phys. Lett. B, 731: 92-96 (2014)

[17] H. Steinwedel, et al., Z. Naturforsch., 5a: 413 (1950)

[18] B. L. Berman, At. Data Nucl. Data Tables, 15: 319-390 (1975)

[19] M. Danos, Nucl. Phys., 5: 23 (1958)

[20] G. Reffo, Phys. Rev. C, 44, 814 (1991)

[21] S. Levinger, Phys. Rev., 84: 43 (1951)

[22] J. S. Levinger, in Nuclear Photo Disintegration (Oxford University Press, Oxford, 1960) p.54

[23] A. Koning et al., TALYS – 1.6 A nuclear reaction program, (2013) p.62

[24] M. Herman et al., EMPIRE – 3.2 Malta modular system for nuclear reaction calculations and nuclear data evaluation, (2013) p.18-20

[25] T. Belgya, et al., Handbook For Calculations of Nuclear Reaction Data, (IAEA, Vienna, RIPL-2, IAEA-TECDOC-1506, 2006), http://www-nds.iaea.org/RIPL-2

[26] V. N. Levkovski, J. Phys., 18: 361 (1974)

[27] J. S. Wang et al., Eur. Phys. J. A, 7: 355-360 (2000)

[28] https://www-nds.iaea.org/exfor/exfor.htm, retrieved 4th December 2015

[29] Akito Takahashi, et al., Fusion Engineering and Design, 9: 323 (1989)

[30] http://www.nndc.bnl.gov/chart/chartNuc.jsp, retrieved 2nd November 2015

[31] https://www-nds.iaea.org/photonuclear/, retrieved 4th December 2015

[32] http://www.nndc.bnl.gov/sigma/index.jsp?dontshow=nn.6&as=9&lib=jendl3.3&nsub=20040, retrieved 4th December 2015

[33] Grady Hughes, Progress in Nuclear Science and Technology, 4: 454-458 (2014)

[34] X-5 Monte Carlo Team, MCNP-A General Monte Carlo N-Particle Transport Code, Version 5, (2000) 1

[35] A. Fassò, et al., Advanced Monte Carlo for Radiation Physics, Particle Transport Simulation and Applications, in Proceedings of the Monte Carlo 2000 Conference, edited by A. Kling, et. al., (Lisbon, 2000) 159-164

[36] P. K. Sahani et al., Indian J. Pure Appl. Phys, 50: 863-866 (2012)

[37] Boubaker Askri, Nucl. Instrum. Methods Phys. Res., Sect. B, 360: 1-8 (2015)